Development 135, 1097-1106 (2008) doi:10.1242/dev.013086

Notochord-derived Shh concentrates in close association with the apically positioned basal body in neural target cells and forms a dynamic gradient during neural patterning

Chester E. Chamberlain*, Juhee Jeong†, Chaoshe Guo‡, Benjamin L. Allen and Andrew P. McMahon§

Sonic hedgehog (Shh) ligand secreted by the notochord induces distinct ventral cell identities in the adjacent neural tube by a concentration-dependent mechanism. To study this process, we genetically engineered mice that produce bioactive, fluorescently labeled Shh from the endogenous locus. We show that Shh ligand concentrates in close association with the apically positioned basal body of neural target cells, forming a dynamic, punctate gradient in the ventral neural tube. Both ligand lipidation and target field response influence the gradient profile, but not the ability of Shh to concentrate around the basal body. Further, subcellular analysis suggests that Shh from the notochord might traffic into the neural target field by means of an apical-to-basal-oriented microtubule scaffold. This study, in which we directly observe, measure, localize and modify notochord-derived Shh ligand in the context of neural patterning, provides several new insights into mechanisms of Shh morphogen action.

KEY WORDS: Shh, Morphogen, Neural tube pattern, Basal body, Primary cilium

INTRODUCTION

Neurons of the vertebrate central nervous system (CNS) are organized into anatomically and functionally distinct domains that allow for the higher-order functions of the brain and spinal cord (Jessell, 2000). The developing spinal cord, or neural tube, begins as a folded sheet of neural progenitor cells that is induced and patterned into spatially distinct domains by adjacent dorsal and ventral organizing centers: the non-neural ectoderm and notochord, respectively. Sonic hedgehog (Shh), a member of the Hedgehog (Hh) family of secreted signaling proteins, mediates the long-range patterning activity of the notochord and specifies five discrete domains of neural progenitors and a second organizing center of Shh activity within the non-neuronal floor plate (FP) at the ventral midline of the neural tube (Briscoe and Ericson, 2001; Jessell, 2000; McMahon et al., 2003).

Increasing concentrations of Shh specify progressively more-ventral cell types in chick neural explants (Briscoe et al., 2000). Importantly, FP-deficient *Gli2* mutants only produce Shh from the notochord, but are still capable of specifying all primary Shh-dependent neural progenitor populations, although some are reduced in number (Matise et al., 1998). These findings support a model wherein a graded Shh signaling response to notochord-derived Shh activates a long-range patterning process in the ventral neural tube, resulting in the regional organization of specific neural progenitor types in spatially distinct ventral domains. However, our understanding of the mechanisms that regulate Shh signal distribution and response throughout the patterning process is largely speculative.

To directly visualize Shh during neural tube patterning, we engineered the mouse *Shh* locus to encode a Shh::GFP fusion protein and examined its distribution in conjunction with Shh-mediated patterning of the ventral neural tube. We report that Shh ligand from the notochord forms a dynamic gradient in the neural target field coincident with the emergence of the ventral pattern, and concentrates adjacent to the apically localized basal body of neural progenitors during this process. Further, we provide evidence that Shh might traffic into the neural target field through ventral midline cells via a microtubule scaffold that spans between the Shh-producing notochord and apically located basal body. These results provide fresh insight into the possible mechanisms of Shh signal distribution and transduction during neural tube patterning.

Department of Molecular and Cellular Biology, The Biolabs, Harvard University, 16 Divinity Avenue, Cambridge, MA 02138, USA.

*Present address: 1550 4th St., Room 381, UCSF Mission Bay campus, San Francisco, CA 94143, USA
†Present address: 1550 4th St., Room 282, UCSF Mission Bay campus, San Francisco, CA 94143, USA
‡Present address: Department of Surgery/Urology, Children's Hospital Boston, Harvard Medical School, 300 Longwood Avenue, Boston, MA 02115, USA
§Author for correspondence (e-mail: mcmahon@mcb.harvard.edu)

Accepted 15 December 2007

MATERIALS AND METHODS

Imaging

Fluorescent images were collected using a Zeiss LSM510 confocal microscope. Shh::GFP images used for comparisons were collected and processed identically. Shh::GFP images in figures were background subtracted, level adjusted and low-pass filtered. Background values used in background subtraction were determined from images of stage-matched wild-type neural tubes that had been dissected, fixed and imaged identically. Applying background subtraction on an image collected from a wild-type neural tube results in an image with an average pixel value of zero. Low-pass filtering (2×2 Gaussian) was performed to remove noise, and pixels in displayed images were saturated using the level adjustment feature in Photoshop (Adobe) so that the entire Shh::GFP distribution is clearly visible in figures. Images used for quantifying Shh::GFP were not low-pass filtered and contained no saturated pixels to ensure accurate measurements. Images comparing apical regions were aligned in Photoshop based on ventral midline nuclei. The average pixel intensity of areas within images was measured using ImageJ (NIH) and plotted using Excel (Microsoft). Images were collected using a 63× (1.4 NA) oil-immersion lens and co-localization images were collected using four laser lines (405, 488, 543, 633 nm) at the same optical thickness of 1 μm based on a limiting airy disk diameter of '1' for the 633 nm wavelength. Confocal stacks were collected using 0.35 μm steps along the *z*-axis (an ~3× optical oversampling). The apical region is defined as the space between the most apically positioned nuclei of the ventral neural tube.

Tissue section preparation and staining

Embryos were fixed in 4% paraformaldehyde (Electron Microscopy Sciences) in Dulbecco's phosphate-buffered saline (DPBS; Gibco BRL) for 15 minutes (E9.5 and E10.5) or 10 minutes (E8.5), washed in DPBS containing 0.1 M glycine (DPBS-G) three times for 5 minutes each, cryoprotected 4 hours to overnight in 30% sucrose in DPBS at 4°C,

embedded in OCT compound (Tissue-Tek), frozen on dry ice and stored at –80°C. Frozen sections were cut at 20 μm, immediately placed in cold DPBS, fixed in cold 4% paraformaldehyde in DPBS for 10 minutes, washed in cold DPBS-G three times for 5 minutes each and stored at 4°C. E10.5 embryos were sectioned at the level of the forelimb and E8.5 embryos at the level of the heart. All sections are displayed such that dorsal is at the top and ventral is at the bottom. Antibody staining for homeodomain proteins was performed as described (Jeong and McMahon, 2005). For other antibodies, sections were incubated with primary antibodies in block buffer (3% bovine serum albumin, 1% heat-inactivated sheep serum in DPBS) for 2 hours (room temperature) to overnight (4°C), washed three times in cold DPBS, incubated with secondary antibodies in block buffer for 1 hour (room temperature), washed three times in cold DPBS and mounted in Vectashield hard-set mounting media (Vector Labs) overnight at room temperature. Antibodies and dilutions were as follows: mouse anti-Nkx2.2, -Pax6, -Pax7 1:20 (DSHB), rabbit anti-Olig2 1:5000 (gift of H. Takebayashi, National Institute for Physiological Sciences, Okazaki, Japan), rabbit anti-Nkx6.1 1:3000 (gift of J. Jensen, Hagedorn Research Institute, Gentofte, Denmark), rabbit anti-polaris 1:500 (gift of B. Yoder, University of Alabama, Birmingham, AL), mouse anti-γ-tubulin 1:500 (Sigma), mouse anti-acetylated tubulin 1:2500 (Sigma) and secondary antibodies (Molecular Probes). Nuclei were stained with Hoechst. In situ hybridization was performed according to routine procedures.

Generation of the *Shh::gfp* allele and activation of Wnt1::GFP expression

For the generation of the *Shh::gfp* allele, see Fig. S2 in the supplementary material. A *Shh-gfp::Cre* knock-in allele (Harfe et al., 2004) was used to activate expression of a floxed *Rosa-Wnt1::gfp* in the *Shh*-expressing domain (Carroll et al., 2005).

RESULTS

Shh::GFP activity and distribution

To directly visualize Shh ligand in an in vivo context, we generated mice that produce Shh fused to green fluorescent protein (Shh::GFP) in place of wild-type Shh. GFP was inserted into the Shh protein such that the secreted signaling ligand would retain both GFP and lipid modifications post-processing (Fig. 1A). Biochemical and cellular analysis indicates that Shh::GFP undergoes correct processing, albeit less efficiently, to produce active, bi-lipidated signaling peptides (see Fig. S1 in the supplementary material). Next, we targeted GFP into the endogenous *Shh* locus using homologous recombination in mouse embryonic stem cells to create an allele encoding Shh::GFP protein (*Shh::gfp*) (see Fig. S2 in the supplementary material). Mice heterozygous for *Shh::gfp* are normal and indistinguishable from wild-type littermates. However, mice homozygous for *Shh::gfp* are stillborn and show defects consistent with reduced Shh signaling (see Fig. S3 in the supplementary material). Western analysis of embryos at embryonic day 9.5 (E9.5) suggests that Shh::GFP is produced and correctly processed in vivo, but at reduced levels compared with wild-type Shh protein (see Fig. S3 in the supplementary material). Thus, the failure of *Shh::gfp* to fully complement the *Shh* allele most likely results from a reduction of Shh signaling (see additional evidence below).

Shh acts as a morphogen in ventral patterning of the vertebrate neural tube (Ingham and Placzek, 2006). To assess Shh::GFP patterning activity, we assayed *Shh::gfp* homozygous neural tubes at E10.5 for Shh-dependent neural progenitor domains. All domains

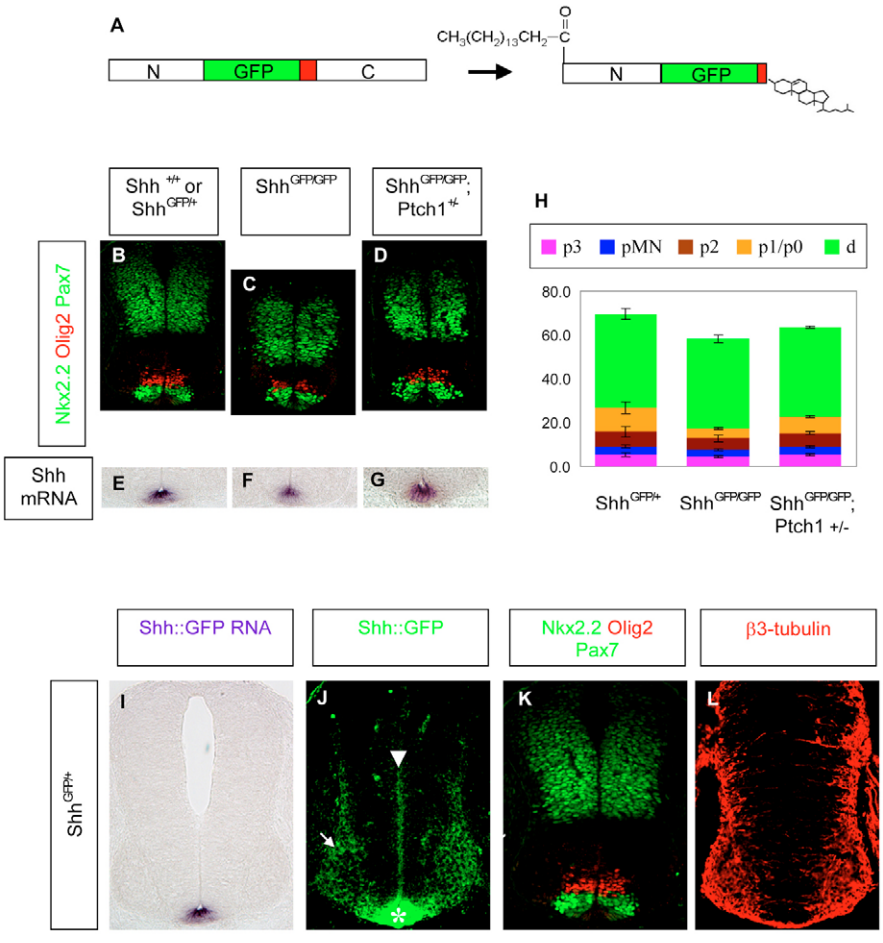

Fig. 1. Shh::GFP activity and distribution in the mouse neural tube. (**A**) Diagram of full-length and processed Shh::GFP. The Shh processing site is disrupted by GFP insertion and a new processing site is added after the GFP (red) so that processing releases an N-terminal fragment that is GFP tagged. (**B-H**) Shh::GFP specifies all Shh-dependent ventral cell identities. (B-D) Analysis of Shh-dependent neural progenitors in E10.5 spinal cord regions of embryos with indicated genotypes. Immunostaining with ventral-specific markers to identify ventral progenitor domains: Nkx2.2 (p3, lower green), Olig2 (pMN, red), and Pax7 (dorsal progenitors, upper green). (E-G) In situ hybridization for *Shh* RNA in E10.5 neural tube sections of embryos with indicated genotypes at the spinal cord level. (H) Quantification of the size of each progenitor domain (p3, pMN, p2, p1/p0, d) along the D-V axis in cell diameters in $Shh^{GFP/+}$, $Shh^{GFP/GFP}$ and $Shh^{GFP/GFP}$;$Ptch1^{+/-}$ neural tube sections at the level of the forelimb (E10.5). Values represent the average from two sections per embryo across three embryos of a given genotype. (**I-L**) Neural tube cross-sections of $Shh^{GFP/+}$ embryos at E10.5 (dorsal is up and ventral down). (I) *Shh* and *Shh::gfp* expression visualized by RNA in situ hybridization. (J) Shh::GFP distribution directly visualized by confocal microscopy. Shh::GFP protein at the expressing floor plate (*), responding progenitor (below the arrowhead) and non-responding mantle (arrow) domains. (K) Immunostaining of Shh-dependent neural progenitor domains p3 (Nkx2.2, green) and pMN (Olig2, red) in the ventricular region. Pax7 is repressed by low-level Shh signaling and is restricted to dorsal neural precursors (green). (L) Immunostaining of post-mitotic neurons (β3-tubulin, red).

were present in their correct relative position, although some were reduced in size (Fig. 1B-D,H). In addition, *Shh::gfp* was expressed at the ventral midline (Fig. 1E-G), indicating that Shh::GFP induces FP, the cell type known to require the highest level of Shh activity for its specification (Ericson et al., 1997; Marti et al., 1995; Roelink et al., 1995). Importantly, removing one copy of *Ptch1*, a feedback antagonist of Hh signaling that sequesters ligand, significantly normalized the size of each neural progenitor domain (Fig. 1H) and the gross phenotype of *Shh::gfp* homozygous embryos (see Fig. S3 in the supplementary material), consistent with the view that GFP modification results in reduced levels of Shh ligand with normal bioactivity.

To determine whether Shh::GFP distribution was generally comparable to wild-type protein, we examined Shh::GFP directly in sections of E10.5 neural tubes using confocal microscopy. As expected, the levels of Shh::GFP were highest at the FP where *Shh* is normally expressed (Fig. 1I,J). Shh::GFP outside the production domain (hereafter referred to as Shh::GFP ligand) was detected at the ventricular region of responding neural progenitors and at the mantle region of non-responsive, post-mitotic neurons (arrowhead and arrow in Fig. 1J), consistent with the distribution of endogenous Shh protein reported in an earlier study (Gritli-Linde et al., 2001). Together, our data indicate that Shh::GFP supports Shh morphogen-based patterning of the ventral neural tube and has a similar distribution to the wild-type signaling protein in the context of ventral neural tube patterning.

In order to correlate the distribution of Shh::GFP ligand with Shh-dependent patterning, we focused all subsequent analyses on *Shh::gfp* homozygous embryos, though generally similar results were observed in more-limited studies of heterozygous embryos (data not shown).

Shh::GFP ligand from the notochord establishes a gradient at the apical region of ventral progenitors

All Shh-dependent progenitor domains are established and the notochord has regressed by E10.5. Therefore, we examined the Shh::GFP ligand distribution at earlier stages when active ventral neural patterning is occurring. At E8.5 and E9.5, the notochord is in direct contact with the basal surface of the neural tube at the ventral midline and Shh-dependent patterning has initiated but is not complete (Fig. 2G,H). As expected, *Shh::gfp* expression was restricted to the notochord at E8.5 (Fig. 2A), but was observed in the notochord and at the ventral midline of the neural tube at E9.5 (Fig. 2B). Whereas Shh::GFP ligand was detected both apically (towards the lumen) and basolaterally at E9.5 (Fig. 2E), Shh::GFP ligand was only detected apically at E8.5, when Shh derives exclusively from the notochord (Fig. 2D). As GFP detection may be more sensitive than RNA detection, we examined the Shh::GFP distribution in *Gli2* mutant neural tubes, which lack the Shh-expressing FP population (Matise et al., 1998), to determine whether the apically localized ligand at E8.5 might reflect low-level expression of *Shh::gfp* within ventral midline neural progenitors. As expected, *Shh::gfp* expression was confined to the notochord of *Gli2* mutant neural tubes (Fig. 2C), whereas active patterning was observed over several cell diameters (Fig. 2I). Strikingly, Shh::GFP ligand was only detected in the apical compartment of target cells (Fig. 2F), as in E8.5 embryos that have wild-type Gli2 function (Fig. 2D). Thus, Shh::GFP ligand from the notochord concentrates within an apical subcompartment of neural progenitors coincident with the specification of ventral cell identities. Importantly, immunodetection of wild-type Shh protein with an antibody indicated that the distribution of Shh::GFP ligand reflects the normal distribution of secreted, wild-type Shh protein (Fig. 2J).

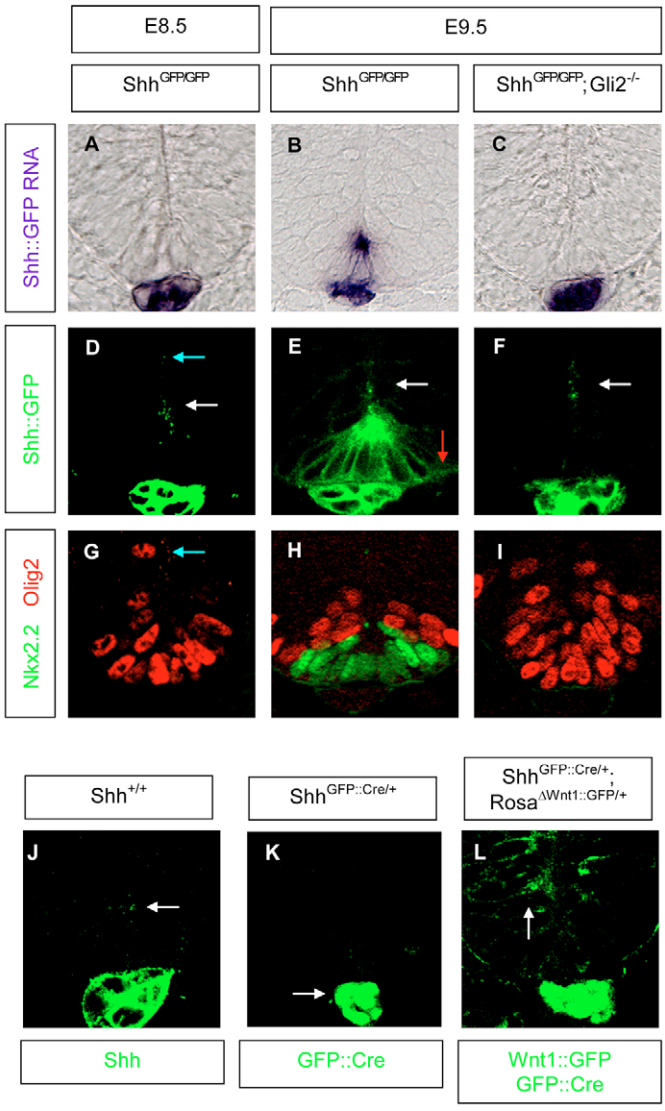

Fig. 2. Notochord-derived Shh::GFP ligand concentrates at the apical region of the neural tube. Neural tube sections of embryos of genotypes and stages indicated. (**A-C**) *Shh::gfp* expression visualized by RNA in situ hybridization. (**D-F**) Shh::GFP distribution directly visualized by confocal microscopy. Shh::GFP concentrated in an apical region of ventral midline cells overlying the notochord (white arrows in D-F) and basolateral region (red arrow, E). (**G-I**) Immunostaining showing Shh-dependent neural progenitor domains p3 (Nkx2.2) and pMN (Olig2). (**J**) Immunostaining for Shh in wild-type mouse embryos using an Shh antibody. Note apical signal (arrow). (**K**,**L**) A *Shh*-driven GFP::Cre transgene (*Shh*$^{GFP:::Cre}$) (Harfe et al., 2004) is only detected in the Shh-expressing notochord (arrow in K). Wnt1::GFP, following ShhGFP::Cre-mediated activation of a ubiquitous *Wnt1::gfp* expression allele (Carroll et al., 2005) specifically in the notochord, is detected in the neural tube (arrow in L). Note that the most dorsally positioned Shh::GFP ligand signal in D is punctate and is adjacent to the most dorsally positioned pMN cell in G (blue arrows).

To determine whether the target field accumulation of ligand was a general property of a protein secreted by the notochord or a more specific property of Shh, we activated *Wnt1::gfp* expression in the

notochord and examined the Wnt1::GFP ligand distribution at E8.5 in the overlying neural tube (see Materials and methods). Like Hh proteins, Wnt proteins are secreted lipid-modified signaling ligands (Takada et al., 2006; Willert et al., 2003). Wnt1::GFP is biologically active (Carroll et al., 2005) and Wnt1, along with other Wnt signals, can activate a potent mitogenic response in neural progenitor cells (Dickinson et al., 1994; Megason and McMahon, 2002). In contrast to Shh::GFP, notochord-derived Wnt1::GFP ligand showed no significant apical accumulation. Instead, Wnt1::GFP ligand was broadly distributed on or around ventral progenitor cells (Fig. 2K,L). Thus, the observed apical localization of Shh within its target field is a Shh-specific distribution.

Shh forms a gradient in the neural target field that is restricted by negative feedback and is dependent on ligand lipidation

The bulk of notochord-derived Shh is restricted to the apical region of neural progenitors at E8.5 (8-12 somites) and has a punctate distribution that is spread across several cell diameters (Fig. 2D,G, blue and white arrows). Next, we examined the Shh::GFP ligand distribution in 14- to 15-somite-stage neural tubes, a time when *Shh* expression is restricted to the notochord and at least three ventral progenitor domains (p2, pMN and p3) have been established (Jeong and McMahon, 2005). The amount of Shh::GFP ligand was found to be increased in the ventral neural tube, but continued to be predominantly apical in neural progenitors (Fig. 3D). High magnification of the apical region revealed that small, individual puncta could still be resolved at a dorsal position (Fig. 3G, white arrow), as in 8- to 12-somite-stage neural tubes (Fig. 2D). However, Shh::GFP ligand at a more ventral position formed one large punctate mass, presumably as a result of several overlapping smaller puncta in this region (Fig. 3G, red arrow).

Next, we plotted the Shh::GFP ligand distribution within the apical region along the dorsal-ventral (D-V) axis beginning at the apical surface of ventral midline cells (Fig. 3J). Shh::GFP ligand spanned ~25 μm, crossing five cell diameters (5 μm per cell). Mapping the position of Shh-dependent ventral progenitor domains present at this time (p3, pMN and p2), we found that the concentrated ligand is highest at p3, drops rapidly across pMN and then slowly disappears across p2. Thus, apically concentrated Shh::GFP ligand extends as a gradient that drops exponentially along the D-V axis, spanning three Shh-dependent cell types.

Shh morphogen activity in the neural tube is regulated by a partially redundant, Shh-induced negative-feedback mechanism that acts to bind and sequester Shh ligand at the cell surface (Jeong and McMahon, 2005). To determine whether the target field gradient is also regulated by negative-feedback mechanisms, we quantified the Shh::GFP ligand distribution in smoothened (*Smo*) mutant neural tubes, where all Hh-responsiveness is lost (Zhang et al., 2001). As expected, *Smo* neural tubes lacked Shh-dependent ventral progenitors (Fig. 3A,B). However, Shh::GFP ligand continued to concentrate within the apical region of target cells (Fig. 3D,E), suggesting that this distribution is feedback-independent. However, the Shh::GFP ligand distribution in *Smo* mutant neural tubes became generally less restricted. Significant ligand accumulation was observed on, or close to, the cell surface of neural progenitors, reminiscent of the distribution observed in non-responsive neurons within the mantle region in the E10.5 neural tube (arrow in Fig. 1J) and that observed for notochord-derived Wnt1::GFP ligand (Fig. 2K).

Quantitative analysis of the apical target field distribution indicated that the gradient spans over 60 μm (or twelve cell diameters) in the absence of *Smo* function, approximately twice

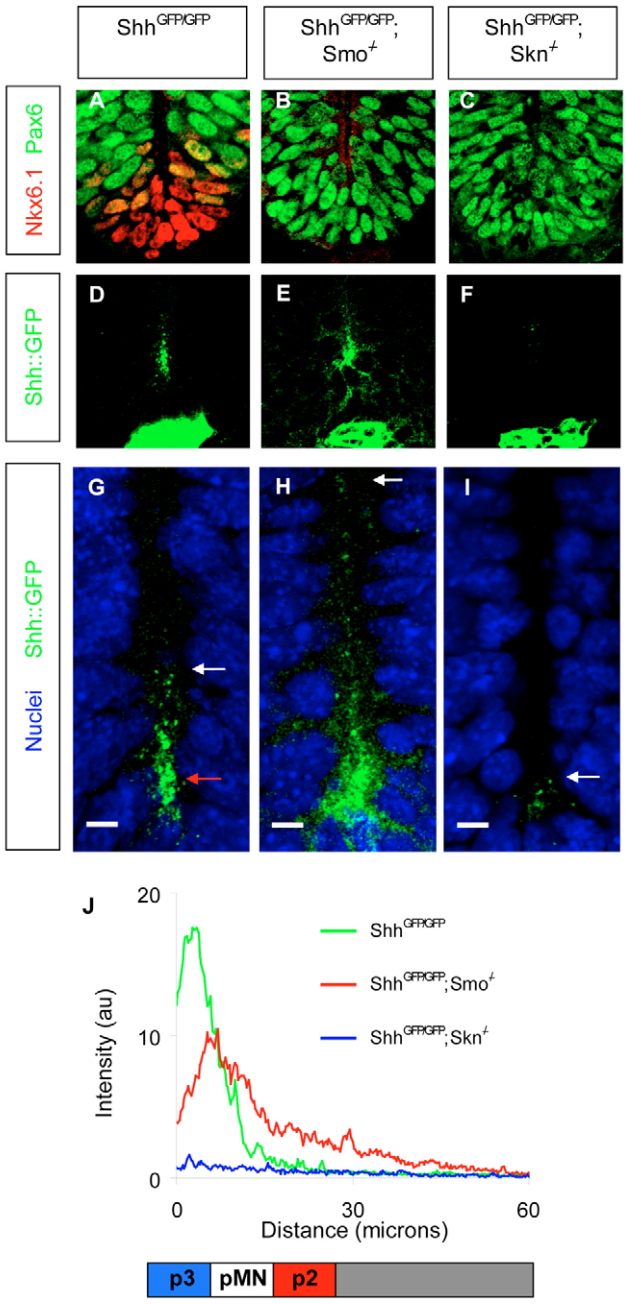

Fig. 3. Shh::GFP ligand forms a gradient at the apical region that can be modified by *Smo* and *Skn* activity. (**A-I**) Sections of 14- to 15-somite-stage mouse neural tubes of indicated genotypes. (A-C) Immunostaining for Nkx6.1, whose expression is activated by Shh signaling, and for Pax6, whose expression is repressed by Shh signaling in the ventral neural tube. (D-F) Shh::GFP ligand distribution directly visualized by confocal microscopy. (G-I) High magnification of the apical, ventral neural tube. Images are a projection of six confocal images taken sequentially along the *z*-axis compressed into one to provide a better sampling of the total Shh::GFP ligand distribution. Note that Shh::GFP ligand forms a large punctum near the ventral midline (G, red arrow) at this stage that is presumably made up of several smaller puncta. White arrows indicate approximate dorsal limit of detectable Shh::GFP ligand. (**J**) Profiles of apical Shh::GFP ligand along the D-V axis of indicated genotypes. Profile represents an average based on two sections per embryo across three embryos. Approximate positions of Shh-dependent progenitors p3, pMN and p2 in a $Shh^{GFP/GFP}$ neural tube at this stage are displayed along the *x*-axis. Scale bars: 5 μm in G-I.

as far dorsally as ligand in neural tubes where Smo-dependent feedback processes are operative (Fig. 3G,H,J). Further, the spatial profile of ligand distribution along the D-V axis was altered. Instead of dropping exponentially, Shh::GFP ligand in *Smo* mutant neural tubes displayed a linear profile across the ventral neural target field (Fig. 3J). Thus, Smo, and consequently Hh-responsiveness, is not required for Shh::GFP ligand to concentrate in its normal apical domain but feedback mechanisms are likely to prevent ligand from concentrating more generally on or around neural progenitors. In addition, a negative-feedback mechanism restricts the range and dictates the shape of the gradient consistent with the previous description of Ptch1 and Hip1 feedback mutants (Jeong and McMahon, 2005), demonstrating that the target field gradient is clearly linked to Shh morphogen activity.

Next, we examined the significance of N-terminal lipid modification on the Shh::GFP ligand distribution. skinny hedgehog [*Skn*; also known as hedgehog acyltransferase (*Hhat*)] encodes an enzyme that palmitoylates Shh ligand on an N-terminal cysteine residue. This lipid modification has been suggested to critically regulate Shh activity and, consequently, Shh-dependent specification of ventral cell fates (Chen et al., 2004; Kohtz et al., 2001; Pepinsky et al., 1998). Direct analysis of Shh::GFP in E8.75 *Skn* mutant neural tubes (Fig. 3C,I,J) demonstrated dramatically reduced levels of protein in target cells. A significant accumulation of Shh::GFP ligand could only be detected in midline neural progenitors that contact the notochord. Significantly, Shh::GFP ligand was apically localized within these cells (Fig. 3I). As *Skn* mutants display a markedly different distribution from *Smo* mutants, the reduction of concentrated Shh::GFP ligand is unlikely to simply reflect a loss of responsiveness within the neural target field to non-palmitoylated Shh ligand. More likely, this reflects a failure of cell-surface proteins to bind or traffic non-palmitoylated Shh::GFP ligand in vivo. In addition, no obvious difference in Shh::GFP production was observed in the notochord between each class of mutant embryo. Thus, the observed changes in Shh::GFP ligand distribution in *Smo* and *Skn* mutants provide strong genetic evidence that the observed target field distribution is related to the morphogen-based patterning activities of Shh.

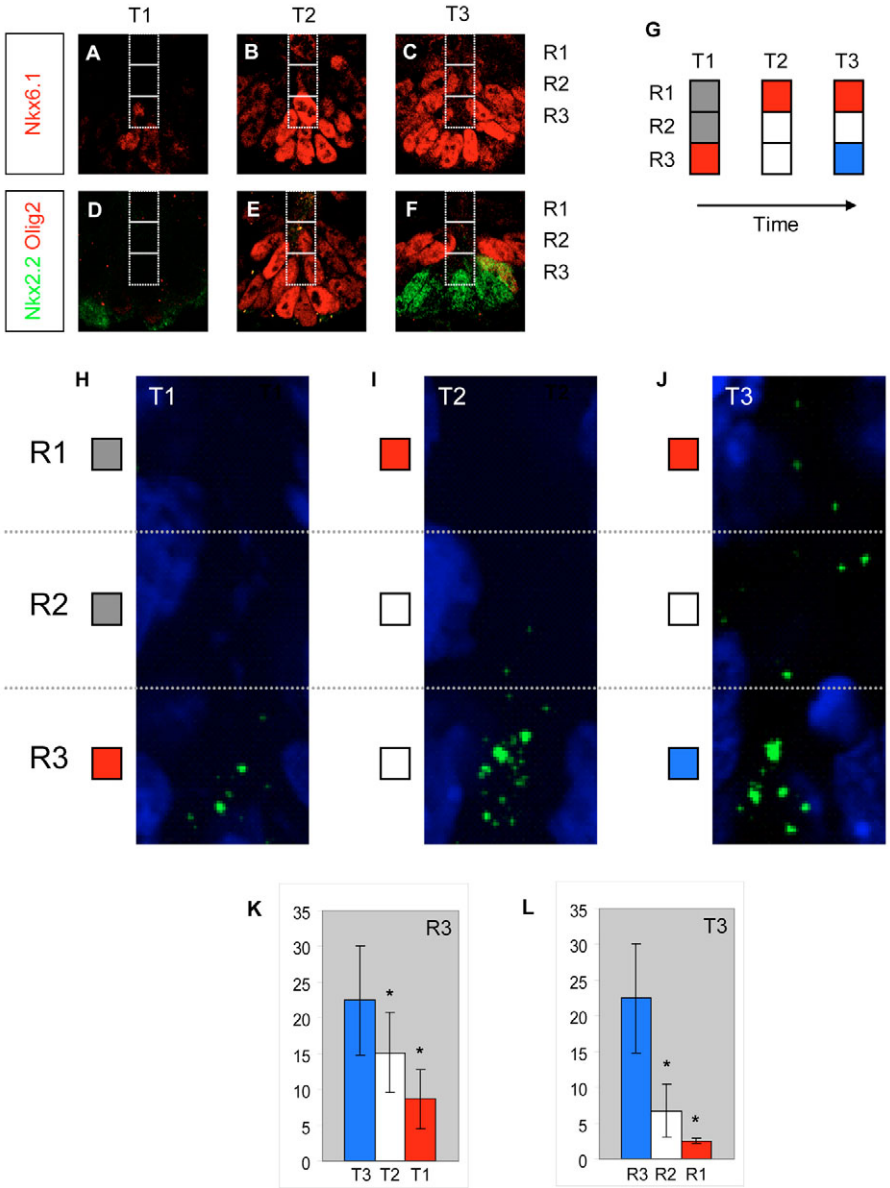

Fig. 4. Shh::GFP ligand distribution during the emergence of ventral pattern. (**A-F**) Sections of 6- to 12-somite-stage mouse ventral neural tubes were analyzed at three developmental time points as determined by the appearance of distinct ventral cell types at the ventral midline (T1, p2; T2, pMN; T3, p3). (**G**) Schematic showing the changes in domain state across three distinct regions (R1-R3) of ventral neural tube. Each region represents a 9 μm × 9 μm square along the D-V axis with R3 beginning at the apical region of ventral midline cells. Red, p3; white, pMN; blue, p2. (**H-J**) Single confocal sections of ventral neural tube at the apical region (Shh::GFP ligand, green; nuclei, blue). (**K**,**L**) Quantitation of Shh::GFP ligand intensity (*y*-axis, average pixel intensity) at different time points and regions. Each time point represents four sections from three embryos. Significant differences from R3 are indicated by asterisks [*P*-values: T3(R3,R2), $P<0.0298$; T3(R2,R1), $P<0.1275$; T3(R1,R3), $P<0.0125$; R3(T3,T2), $P<0.0417$; R3(T2,T1), $P<0.0775$; R3(T3,T1), $P<0.0458$].

However, neither appropriate lipid modification nor Shh responsiveness is absolutely required for Shh ligand to accumulate at the apical region of cells in the target field.

A temporal gradient of Shh ligand at the ventral midline

We observed that Shh::GFP ligand forms a gradient across Shh-dependent ventral cell types, consistent with a long-range mechanism for Shh morphogen action. Further, our analysis suggests that the target field gradient is sensitive to both negative feedback and Skn-mediated palmitoylation. However, the Shh-dependent pattern of ventral neural progenitors does not emerge at a single time point but instead over time, with a dorsal-to-ventral appearance of cell types at the ventral midline (Jeong and McMahon, 2005). From this, one might expect Shh ligand to quickly establish a long-range gradient across the ventral neural tube so that target cells can acquire positional information. We therefore examined the Shh::GFP ligand distribution when each progenitor cell type first occupied the ventral midline: p2 (T1), pMN (T2) or p3 (T3) in 6- to 12-somite-stage embryos (Fig. 4A-F). To track changes in the spatial distribution of ligand, the apical region of the ventral neural tube was divided into three fixed regions (R1, R2 and R3). R3 covers the apical region associated with ventral midline cells, whereas R2 and R1 cover the apical region of more-dorsally positioned progenitors. When p2 progenitors occupied the ventral midline (T1), Shh::GFP ligand was only detected in region R3 (Fig. 4H). Shh::GFP ligand increased in region R3 when the ventral midline was occupied by pMN progenitors (T2) and expanded dorsally into region R2, where p2 progenitors were now positioned (Fig. 4I). When p3 occupied the ventral midline (T3), Shh::GFP ligand again increased in region R3 and could now be detected in regions R2 and R1, where pMN and p2 progenitors reside, respectively (Fig. 4J). Thus, the target field gradient of Shh::GFP ligand, like the Shh-dependent neural pattern, emerges over time, beginning at the apical region of ventral midline cells and then spreading dorsally. It remains to be determined whether the dorsal movement of Shh::GFP ligand reflects actual ligand movement, or a dorsal expansion of ventral cells that retain Shh::GFP ligand, or both.

Next, we quantified the accumulation of Shh::GFP ligand at the apical region of ventral midline cells (R3) when each progenitor cell type first appeared. We found that the level of Shh ligand progressively increased, forming a temporal gradient at region R3 as ventral cell types emerged (Fig. 4K). However, unlike the exponential gradient spanning the three ventral cell types at T3 (Fig. 4L), the temporal gradient is linear. Although it is not clear which gradient is relevant to Shh morphogen activity, the temporal gradient is more consistent with the profile of Shh concentrations that progressively specify more-ventral cell types in vitro (Ericson et al., 1997).

Shh::GFP ligand concentrates at the base of the primary cilium

Next we sought to identify the subcellular location where Shh::GFP ligand concentrates in target cells. A number of studies have shown that Hh signaling components, including Shh (Rohatgi et al., 2007), can be found at the primary cilium of target cells, although not in the context of active neural patterning (Haycraft et al., 2005; Huangfu and Anderson, 2005; Rohatgi et al., 2007; Scholey and Anderson, 2006; Yoder, 2006). A primary cilium is present on most mammalian cells and is an apical structure in epithelial tissue. Staining for acetylated α-tubulin, a marker for the shaft of the primary cilium (Essner et al., 2002), revealed a dense, complicated network of microtubules at the apical region of the neural tube, preventing an unambiguous identification of the primary cilium in this region (data not shown). The absence of other cilial-specific markers prevented a direct analysis of the primary cilium itself. At the cilial base, a centriole-containing basal body generates the microtubule scaffold supporting the primary cilium, whereas the adjacent transition zone acts as a loading dock for intraflagellar transport (IFT) proteins that traffic cargo to the cilial compartment (Rosenbaum and Witman, 2002; Scholey, 2003). Gamma-tubulin is a component of the basal body, whereas polaris (Ift88) demarcates the transition zone (Haycraft et al., 2005; Taulman et al., 2001). As individual punctate structures can be resolved (Fig. 5A and data not shown), we were able to determine whether Shh::GFP ligand puncta preferentially associate with these structures in the apical region of the ventral neural tube. In addition, we focused our analysis on 8-somite-stage neural tubes as the amount of Shh::GFP ligand in the apical region at later stages is too high for co-localization analysis.

Strikingly, a three-way comparison of γ-tubulin, polaris and Shh::GFP ligand puncta within the apical gradient showed that most (74%) of the Shh::GFP ligand puncta associated (within 1 μm) with

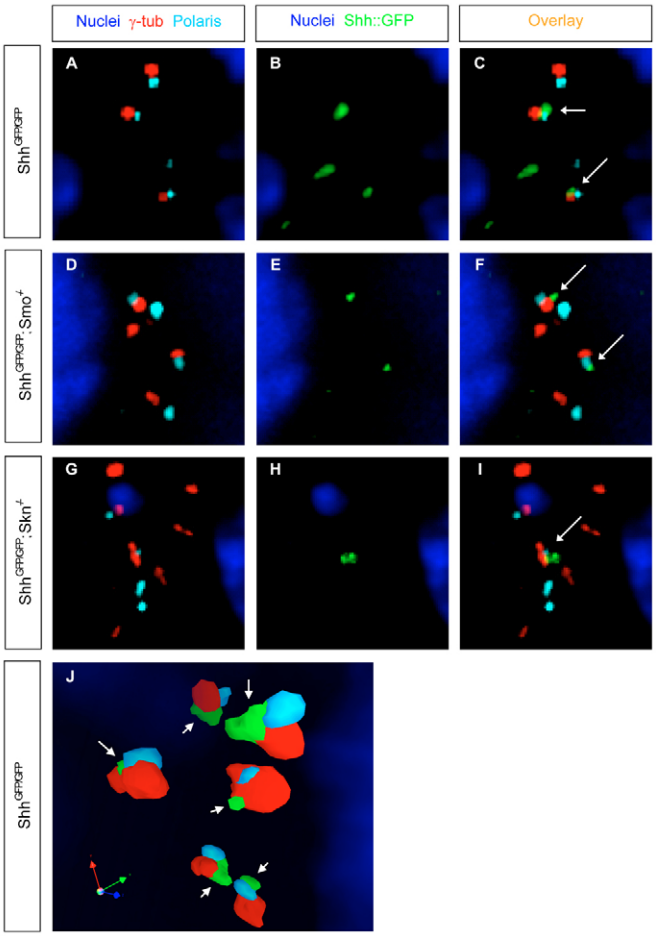

Fig. 5. Subcellular distribution of concentrated Shh::GFP ligand in apical region. (**A-I**) High magnification of apical region in 8-somite-stage mouse neural tubes of indicated genotypes. Nuclei (blue), Shh::GFP ligand (green), γ-tubulin (γ-tub, red), polaris (turquoise). Images are single confocal slices. Association of Shh::GFP ligand, γ-tubulin and polaris is shown by arrows. Shh::GFP ligand continues to associate with the basal body region in *Smo* and *Skn* mutants. (**J**) Three-dimensional surface rendering of six confocal images taken sequentially along the *z*-axis. Note the adjacent, non-overlapping co-localization of the three proteins.

the basal body and transition zone (Fig. 5A-C,J). By contrast, only a small fraction (17%) of Shh::GFP puncta associated with the lysosome, an organelle expected to degrade internalized Shh ligand (Fig. 6A-C). To determine whether there are regional differences in the association of Shh::GFP ligand puncta with the basal body, we quantified the basal body association within three volumes (V1, V2 and V3) along the D-V axis (Fig. 7A). The Shh::GFP/basal body association progressively decreased ventrally (Fig. 7B), with all Shh::GFP ligand puncta associated with the basal body at the most dorsal volume (V1) and only 50% at the most ventral volume (V3). The change in association might be due to differences in the nature of Shh signaling at different D-V positions. Alternatively, there could be temporal differences. For example, cells at the ventral midline might have been exposed to Shh signaling for longer periods of time, allowing negative-feedback components to drive ligand away from the basal body and towards the lysosome for degradation. Regardless, our analysis indicates that the bulk of Shh::GFP ligand within the target field gradient is associated with the apically positioned basal body of neural progenitors during active Shh morphogen-based patterning of the ventral neural tube, a highly asymmetric distribution within target cells. As Shh::GFP ligand can localize to this position in *Smo* and *Skn* mutants (Fig. 5D-I), secondary response-dependent processes are not required or responsible for this specific intracellular distribution.

Shh::GFP ligand between the notochord and target field gradient is associated with microtubules

Although most of the Shh::GFP ligand is detected at the apical region of neural progenitors during early patterning, smaller Shh::GFP puncta are found at more-basal positions within those ventral midline cells directly overlying the Shh::GFP-secreting notochord. Staining for acetylated α-tubulin revealed an extensive microtubule network that spans the apical-to-basal surfaces of ventral midline cells (Fig. 6D). Strings of small Shh::GFP ligand puncta (smaller than the basal-body-associated accumulations) were found in close association with these microtubules (Fig. 6E,F). As this association occurs at stages prior to *Shh::gfp* expression at the ventral midline and in *Gli2* mutant neural tubes (Fig. 6D-F), the small Shh ligand puncta must have originated from the notochord. Thus, these puncta might represent Shh::GFP ligand trafficking from the Shh::GFP-expressing notochord into the neural target field, a process that might be facilitated by the physical contact between these two distinct tissues.

DISCUSSION

Mechanism of Shh morphogen action in neural tube patterning

Shh ligand secreted by the notochord specifies the identity of ventral cell types in the adjacent neural tube through a concentration-dependent mechanism. Several studies to date support a long-range morphogen model to explain Shh action. In the simplest model, Shh ligand establishes a stable long-range gradient across the ventral neural target field, allowing subpopulations of progenitors to acquire unique positional values based on the local concentration of Shh ligand. The positional values are then translated into the expression of specific transcriptional regulators that drive the regional specification of neural identities, resulting in the final neural pattern. However, patterning is a dynamic process and both the concentration of morphogen that a cell is exposed to and the response of a cell to that morphogen are likely to change over time. Thus, the reality of how a cell acquires a positional value is likely to be a complex process.

Clearly, understanding how Shh is distributed as ventral cell fates emerge is crucial to our understanding of this process. To address this question, we replaced the endogenous Shh protein with a fluorescently tagged form in the mouse and visualized its distribution in the context of active neural patterning in vivo. Shh ligand is first detected at the apical region of ventral midline cells

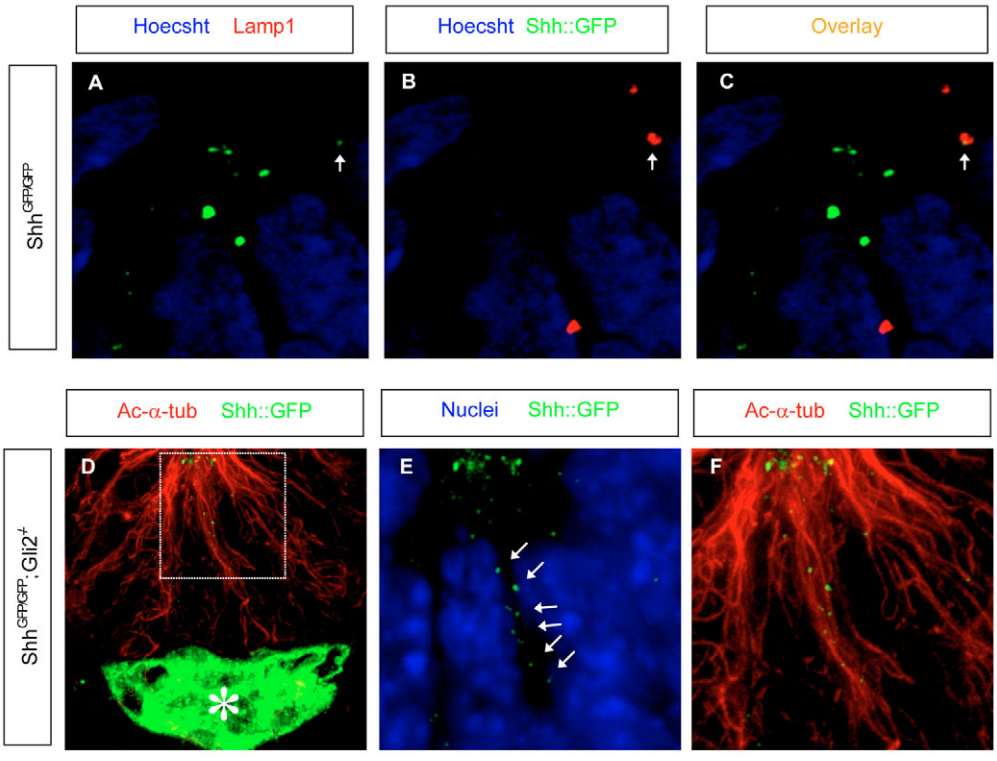

Fig. 6. Association of Shh::GFP ligand with lysosomes and stabilized microtubules. (**A-C**) High magnification of apical compartment of 8-somite-stage mouse neural tubes of indicated genotype. Nuclei (blue), Shh::GFP ligand (green), Lamp1 (red). The association of Shh::GFP ligand with the lysosome is indicated by the arrows. The bulk of Shh::GFP ligand apical accumulation does not co-segregate with the lysosome. (**D-F**) Immunostaining for acetylated α-tubulin reveals a network of stabilized microtubules (red) that span between the apical and basal surfaces of neural progenitors. Shh::GFP (green) is present in the notochord (asterisk). The boxed region in D is shown at high magnification in E,F. Arrows in E indicate a string of Shh::GFP ligand puncta.

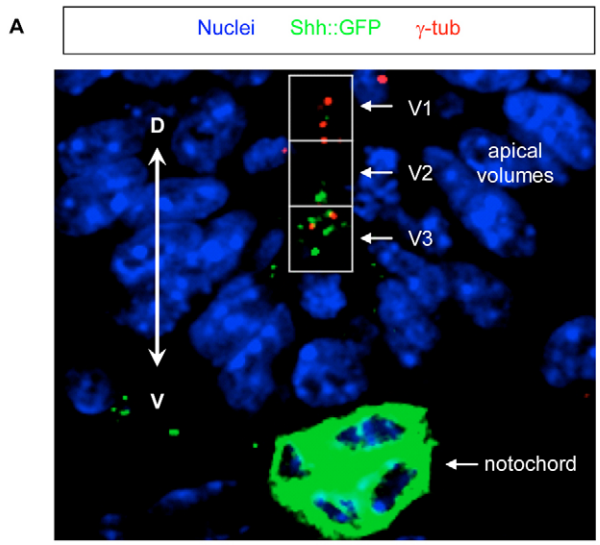

B

	apical volumes		
	V1	V2	V3
Number of Shh::GFP ligand puncta	1 ± 0	3 ± 1	8 ± 2
Number of basal bodies	9 ± 2	10 ± 2	6 ± 4
Number of basal body associated Shh::GFP ligand puncta	1 ± 1	2 ± 1	4 ± 2
Number of associated nuclei	11 ± 2	12 ± 4	22 ± 6
Percentage of Shh::GFP ligand puncta associated with a basal body	100%	67%	50%

Fig. 7. Quantitation of Shh::GFP ligand puncta and basal bodies in early ventral neural tubes. Eight-somite-stage mouse neural tubes cut at the level of the heart were analyzed at three distinct volumes (V1, V2, V3) along the D-V axis. (**A**) The relative positions of V1, V2 and V3 in the *xy*-plane. Each volume is 9 μm wide (*x*-axis), 9 μm long (*y*-axis) and 2.1 μm deep (a stack of six confocal images taken at 0.35 μm steps along the *z*-axis). Nuclei (blue), Shh::GFP ligand (green), γ-tubulin (red). (**B**) Quantification of Shh::GFP ligand puncta and basal bodies within each apical volume. A Shh::GFP punctum is basal-body-associated if it is within 1 μm of a γ-tubulin punctum. A nucleus is associated with an apical volume if it is laterally positioned to that volume. Ventral midline nuclei are associated with V3. Note that the percentage of Shh::GFP puncta associated with the basal body decreases ventrally.

when patterning begins and then extends dorsally as neural patterning progresses (Fig. 4). Thus, the Shh ligand profile in the ventral neural target field does not appear to rapidly reach a steady state, but appears to slowly emerge with the ventral pattern. That the observed target field accumulation is related to Shh morphogen action is supported by the sensitivity of the gradient profile to both negative feedback and Skn-mediated palmitoylation, both of which have been shown to be crucial modulators of Shh morphogen activity in the neural tube (Briscoe et al., 2001; Chen et al., 2004; Jeong and McMahon, 2005).

As Shh acts directly to specify neural progenitors and individual identities are specified by different concentrations of Shh ligand, it is likely that Shh morphogen action reflects a graded signaling mechanism. We therefore investigated the possibility that Shh morphogen activity might be spatially restricted, but temporally distributed, by performing quantitative analysis of ligand accumulation at the ventral midline when distinct ventral cell types first appear. Remarkably, the temporal gradient of Shh ligand accumulation is similar to the in vitro profile of Shh concentrations that specifies progressively more-ventral cell types, showing a ~2- to 3-fold increase between distinct ventral cell identities (Ericson et al., 1997). These data suggest that Shh morphogen activity might be distributed temporally at the ventral midline during neural tube patterning, consistent with a time-based model for Shh-dependent neural patterning (Stamataki et al., 2005). In this model, a specific cell identity may be specified at a precise ventral location where signaling is progressively increasing. However, as cell descendants assume more-dorsal positions in this rapidly dividing tissue, they now enter a new zone where Shh levels may actually decrease to a level insufficient to promote further specification. The relationship between time spent within a specific concentration range of Shh ligand and the locking in of a specific cell fate remains unclear. However, experiments aimed at addressing this might shed light on the in vivo patterning process.

The cilium base and Shh signal transduction

The localization of Shh ligand adjacent to the basal body of target cells is provocative in light of other studies that suggest that the primary cilium plays a role in Hh pathway activation. The primary cilium is found on most cells and is an apical, membrane-bound projection supported by a microtubule scaffold generated by the centriole-containing basal body (Rosenbaum and Witman, 2002). Plus-end (distal) -directed kinesins and minus-end (proximal) -directed dyneins transport cargoes required for the formation, maintenance and function of the primary cilium on its microtubule scaffold. In this, IFT proteins directly bind and traffic these cargoes through the cilial compartment. Ablating IFT genes in the mouse disrupts primary cilium formation and significantly reduces Hh signaling in the neural tube (Huangfu et al., 2003). Genetic epistasis analysis suggests a role for IFT in Gli activity (Haycraft et al., 2005; Huangfu and Anderson, 2005; Liu et al., 2005). Further, cell biological studies suggest that Smo and Ptch1 activity might be restricted to the primary cilium of target cells (Corbit et al., 2005; Rohatgi et al., 2007).

How does the observed accumulation of Shh ligand at the cilium base of target cells fit with the current view of cilium function in Shh signaling? Ptch1 antagonizes Smo in the absence of ligand and Ptch1 appears to be present at the base and within the shaft of the primary cilium (Rohatgi et al., 2007). As Shh can be detected in the shaft when Ptch1::YFP is overexpressed in *Ptch1* mutant MEF cells, it has been proposed that Shh binds and thereby promotes the disappearance of Ptch1 from the primary cilium. The disappearance of Ptch1 is associated with the accumulation of Smo on the primary cilium and with active signaling (Corbit et al., 2005; Rohatgi et al., 2007), although the movement of Ptch1 off the primary cilium is not essential for Smo to function (Rohatgi et al., 2007). Given these findings, it is perhaps surprising that Shh ligand accumulates at the cilium base of neural progenitors during active Hh signaling. However, it is notable that Ptch1 is found predominantly at the cilium base in vivo (Rohatgi et al., 2007). Here, Ptch1 would be well positioned to regulate Smo transport to the primary cilium. Thus, it is possible that Shh ligand traffics to the cilial base and its interaction there with Ptch1 might permit the transport of Smo onto the shaft of the primary cilium to activate the Hh pathway. Reagents that enable the dynamic visualization and spatiotemporal quantification of these crucial signaling components in their physiological contexts will greatly help in understanding these mechanisms. The *Shh::gfp* allele represents the first step in this direction.

Shh target field trafficking

The observed apical accumulation of notochord-derived Shh ligand appears to occur by a Shh-specific mechanism, as notochord-derived Wnt1 ligand has a distinct distribution (Fig. 2L). Several cell-surface, Shh-binding proteins are expressed in the ventral neural tube and may be localized and bound to Shh within the apical compartment of neural progenitors. As the apical gradient of ligand accumulation persists in *Smo* mutant neural tubes, where all Hh signaling is lost, the responsible ligand-binding protein must be present during the primary response of the neural target field to Shh ligand. Several Shh-signal-promoting binding partners have been identified in addition to the primary receptor, Ptch1 (e.g. Gas1, Cdon and Boc) (Allen et al., 2007; Tenzen et al., 2006). Notably, we observe a dramatic reduction in the apical accumulation of non-palmitoylated Shh ligand. As palmitoylation is required for Shh ligand activity, its loss may lead to a reduced association with these binding partners. That Ptch1 accumulates at the base of the primary cilium is consistent with this view (Rohatgi et al., 2007). However, Ptch1 levels are themselves directly related to Shh signaling so there might not be a simple quantitative association between Ptch1 and Shh puncta. We have been unable to directly visualize Ptch1 with available antibodies. Also, the rapid activation of *Shh* expression within neural target cells following loss of Ptch1 activity (Goodrich et al., 1997) (data not shown) prevents notochord-derived Shh::GFP from being visualized in a *Ptch1* mutant background.

How does Shh ligand move into and through the neural target field? Our observations of Shh ligand puncta on stabilized microtubules that span ventral neural progenitors from notochordal to apical surfaces indicate that Shh might be endocytosed and subsequently trafficked through the cell to its site of apical accumulation. Trafficking of protein from the basolateral to apical surfaces of epithelial cells, or transcytosis, occurs in several physiological contexts (Tuma and Hubbard, 2003) and would provide an elegant method of regulating the distribution of Shh signals.

At present, the resolution of microscopy does not enable us to unambiguously determine whether these smaller puncta are in, on, or between cells. Further, the dorsal extension of Shh ligand distribution within the neural target field could occur by a similar mechanism to that regulating uptake in the ventral midline cells, through the apical release of Shh ligand into the lumen of the neural tube, or through the cell division and growth of ventral midline cells such that daughter cells carry with them Shh ligand acquired at a more ventral position. Resolving the mechanisms that contribute to the temporal gradient of Shh ligand will require dynamic approaches to visualize morphogen action.

We thank K. Anderson and B. Yoder for reagents and insightful discussion. *Gli2* and *Skn* mutant mice were generous gifts from A. Joyner and P. T. Chuang, respectively. We thank R. Segal and J. Chan for assistance with the Shh oligomerization assay; J. Lee, T. Mitchison, R. Segal, A. Schier, W. Wei and our colleagues in the McMahon laboratory for helpful advice and comments on the manuscript; D. Smith for assistance with confocal microscopy; R. Schalek for help with SEM; H. Alcorn, T. J. Carroll and H. Tian for technical assistance. B.L.A. was the recipient of a postdoctoral fellowship from the American Cancer Society. This work was supported by an NIH grant (R37 NS033642) to A.P.M.

Supplementary material

Supplementary material for this article is available at
http://dev.biologists.org/cgi/content/full/135/6/1097/DC1

References

Allen, B. L., Tenzen, T. and McMahon, A. P. (2007). The Hedgehog-binding proteins Gas1 and Cdo cooperate to positively regulate Shh signaling during mouse development. *Genes Dev.* **21**, 1244-1257.

Briscoe, J. and Ericson, J. (2001). Specification of neuronal fates in the ventral neural tube. *Curr. Opin. Neurobiol.* **11**, 43-49.

Briscoe, J., Pierani, A., Jessell, T. M. and Ericson, J. (2000). A homeodomain protein code specifies progenitor cell identity and neuronal fate in the ventral neural tube. *Cell* **101**, 435-445.

Briscoe, J., Chen, Y., Jessell, T. M. and Struhl, G. (2001). A hedgehog-insensitive form of patched provides evidence for direct long-range morphogen activity of sonic hedgehog in the neural tube. *Mol. Cell* **7**, 1279-1291.

Carroll, T. J., Park, J. S., Hayashi, S., Majumdar, A. and McMahon, A. P. (2005). Wnt9b plays a central role in the regulation of mesenchymal to epithelial transitions underlying organogenesis of the mammalian urogenital system. *Dev. Cell* **9**, 283-292.

Chen, M. H., Li, Y. J., Kawakami, T., Xu, S. M. and Chuang, P. T. (2004). Palmitoylation is required for the production of a soluble multimeric Hedgehog protein complex and long-range signaling in vertebrates. *Genes Dev.* **18**, 641-659.

Corbit, K. C., Aanstad, P., Singla, V., Norman, A. R., Stainier, D. Y. and Reiter, J. F. (2005). Vertebrate Smoothened functions at the primary cilium. *Nature* **437**, 1018-1021.

Dickinson, M. E., Krumlauf, R. and McMahon, A. P. (1994). Evidence for a mitogenic effect of Wnt-1 in the developing mammalian central nervous system. *Development* **120**, 1453-1471.

Ericson, J., Briscoe, J., Rashbass, P., van Heyningen, V. and Jessell, T. M. (1997). Graded sonic hedgehog signaling and the specification of cell fate in the ventral neural tube. *Cold Spring Harb. Symp. Quant. Biol.* **62**, 451-466.

Essner, J. J., Vogan, K. J., Wagner, M. K., Tabin, C. J., Yost, H. J. and Brueckner, M. (2002). Conserved function for embryonic nodal cilia. *Nature* **418**, 37-38.

Goodrich, L. V., Milenkovic, L., Higgins, K. M. and Scott, M. P. (1997). Altered neural cell fates and medulloblastoma in mouse patched mutants. *Science* **277**, 1109-1113.

Gritli-Linde, A., Lewis, P., McMahon, A. P. and Linde, A. (2001). The whereabouts of a morphogen: direct evidence for short- and graded long-range activity of hedgehog signaling peptides. *Dev. Biol.* **236**, 364-386.

Harfe, B. D., Scherz, P. J., Nissim, S., Tian, H., McMahon, A. P. and Tabin, C. J. (2004). Evidence for an expansion-based temporal Shh gradient in specifying vertebrate digit identities. *Cell* **118**, 517-528.

Haycraft, C. J., Banizs, B., Aydin-Son, Y., Zhang, Q., Michaud, E. J. and Yoder, B. K. (2005). Gli2 and Gli3 localize to cilia and require the intraflagellar transport protein polaris for processing and function. *PLoS Genet.* **1**, e53.

Huangfu, D. and Anderson, K. V. (2005). Cilia and Hedgehog responsiveness in the mouse. *Proc. Natl. Acad. Sci. USA* **102**, 11325-11330.

Huangfu, D., Liu, A., Rakeman, A. S., Murcia, N. S., Niswander, L. and Anderson, K. V. (2003). Hedgehog signalling in the mouse requires intraflagellar transport proteins. *Nature* **426**, 83-87.

Ingham, P. W. and Placzek, M. (2006). Orchestrating ontogenesis: variations on a theme by sonic hedgehog. *Nat. Rev. Genet.* **7**, 841-850.

Jeong, J. and McMahon, A. P. (2005). Growth and pattern of the mammalian neural tube are governed by partially overlapping feedback activities of the hedgehog antagonists patched 1 and Hhip1. *Development* **132**, 143-154.

Jessell, T. M. (2000). Neuronal specification in the spinal cord: inductive signals and transcriptional codes. *Nat. Rev. Genet.* **1**, 20-29.

Kohtz, J. D., Lee, H. Y., Gaiano, N., Segal, J., Ng, E., Larson, T., Baker, D. P., Garber, E. A., Williams, K. P. and Fishell, G. (2001). N-terminal fatty-acylation of sonic hedgehog enhances the induction of rodent ventral forebrain neurons. *Development* **128**, 2351-2363.

Liu, A., Wang, B. and Niswander, L. A. (2005). Mouse intraflagellar transport proteins regulate both the activator and repressor functions of Gli transcription factors. *Development* **132**, 3103-3111.

Marti, E., Bumcrot, D. A., Takada, R. and McMahon, A. P. (1995). Requirement of 19K form of Sonic hedgehog for induction of distinct ventral cell types in CNS explants. *Nature* **375**, 322-325.

Matise, M. P., Epstein, D. J., Park, H. L., Platt, K. A. and Joyner, A. L. (1998). Gli2 is required for induction of floor plate and adjacent cells, but not most ventral neurons in the mouse central nervous system. *Development* **125**, 2759-2770.

McMahon, A. P., Ingham, P. W. and Tabin, C. J. (2003). Developmental roles and clinical significance of hedgehog signaling. *Curr. Top. Dev. Biol.* **53**, 1-114.

Megason, S. G. and McMahon, A. P. (2002). A mitogen gradient of dorsal midline Wnts organizes growth in the CNS. *Development* **129**, 2087-2098.

Pepinsky, R. B., Zeng, C., Wen, D., Rayhorn, P., Baker, D. P., Williams, K. P., Bixler, S. A., Ambrose, C. M., Garber, E. A., Miatkowski, K. et al. (1998). Identification of a palmitic acid-modified form of human Sonic hedgehog. *J. Biol. Chem.* **273**, 14037-14045.

Roelink, H., Porter, J. A., Chiang, C., Tanabe, Y., Chang, D. T., Beachy, P. A. and Jessell, T. M. (1995). Floor plate and motor neuron induction by different concentrations of the amino-terminal cleavage product of sonic hedgehog autoproteolysis. *Cell* **81**, 445-455.

Rohatgi, R., Milenkovic, L. and Scott, M. P. (2007). Patched1 regulates hedgehog signaling at the primary cilium. *Science* **317**, 372-376.

Rosenbaum, J. L. and Witman, G. B. (2002). Intraflagellar transport. *Nat. Rev. Mol. Cell Biol.* **3**, 813-825.
Scholey, J. M. (2003). Intraflagellar transport. *Annu. Rev. Cell Dev. Biol.* **19**, 423-443.
Scholey, J. M. and Anderson, K. V. (2006). Intraflagellar transport and cilium-based signaling. *Cell* **125**, 439-442.
Stamataki, D., Ulloa, F., Tsoni, S. V., Mynett, A. and Briscoe, J. (2005). A gradient of Gli activity mediates graded Sonic Hedgehog signaling in the neural tube. *Genes Dev.* **19**, 626-641.
Takada, R., Satomi, Y., Kurata, T., Ueno, N., Norioka, S., Kondoh, H., Takao, T. and Takada, S. (2006). Monounsaturated fatty acid modification of Wnt protein: its role in Wnt secretion. *Dev. Cell* **11**, 791-801.
Taulman, P. D., Haycraft, C. J., Balkovetz, D. F. and Yoder, B. K. (2001). Polaris, a protein involved in left-right axis patterning, localizes to basal bodies and cilia. *Mol. Biol. Cell* **12**, 589-599.
Tenzen, T., Allen, B. L., Cole, F., Kang, J. S., Krauss, R. S. and McMahon, A. P. (2006). The cell surface membrane proteins Cdo and Boc are components and targets of the Hedgehog signaling pathway and feedback network in mice. *Dev. Cell* **10**, 647-656.
Tuma, P. L. and Hubbard, A. L. (2003). Transcytosis: crossing cellular barriers. *Physiol. Rev.* **83**, 871-932.
Willert, K., Brown, J. D., Danenberg, E., Duncan, A. W., Weissman, I. L., Reya, T., Yates, J. R., 3rd and Nusse, R. (2003). Wnt proteins are lipid-modified and can act as stem cell growth factors. *Nature* **423**, 448-452.
Yoder, B. K. (2006). More than just the postal service: novel roles for IFT proteins in signal transduction. *Dev. Cell* **10**, 541-542.
Zhang, X. M., Ramalho-Santos, M. and McMahon, A. P. (2001). Smoothened mutants reveal redundant roles for Shh and Ihh signaling including regulation of L/R symmetry by the mouse node. *Cell* **106**, 781-792.